2012

HFO1234yf Condensation Inside A Brazed Plate Heat Exchanger

Giovanni A. Longo
tony@gest.unipd.it

Claudio Zilio

HFO1234yf Condensation Inside a Brazed Plate Heat Exchanger

Giovanni A. LONGO*, Claudio ZILIO

University of Padova, Department of Management and Engineering,
Str.lla S.Nicola No.3, I-36100 Vicenza, Italy
Phone: +39 0444 998726 Fax: +39 0444 998888 E-mail: tony@gest.unipd.it

ABSTRACT

This paper presents the heat transfer coefficients and the pressure drop measured during HFO1234yf condensation inside a brazed plate heat exchanger: the effects of saturation temperature, refrigerant mass flux and vapour super-heating are investigated. The heat transfer coefficients show weak sensitivity to saturation temperature and great sensitivity to refrigerant mass flux. At low refrigerant mass flux (< 20 kg/m^{2}s) the heat transfer coefficients are not dependent on mass flux and condensation is controlled by gravity. For higher refrigerant mass flux (> 20 kg/m^{2}s) the heat transfer coefficients depend on mass flux and forced convection condensation occurs. The condensation heat transfer coefficients of super-heated vapour are from 8 to 11% higher than those of saturated vapour. The frictional pressure drop shows a linear dependence on the kinetic energy per unit volume of the refrigerant flow and therefore a quadratic dependence on the refrigerant mass flux. HFO1234yf exhibits heat transfer coefficients lower (10-12%) and frictional pressure drop lower (10-20%) than those of HFC134a under the same operating conditions.

1. INTRODUCTION

All commonly used Hydro-Fluoro-Carbon (HFC) refrigerants have a high Global Warming Potential (GWP), higher than 1000, and some countries have already enacted legislative measures towards a limitation in the use or a gradual phase-out of HFC. The European Union has approved a new directive that bans refrigerants with a GWP over 150 in all new mobile air conditioning systems within 2017 with a phase-out period starting January 1, 2011.
HFO1234yf has been identified as a new low GWP refrigerant, which has the potential to be a global sustainable solution particularly for automotive air conditioning and it is currentl under scrutiny as the working fluid for different applications. HFO1234yf is a pure compound, which exhibits a GWP around 4 and low toxicity and can be used in systems currently designed for HFC134a with minimal modifications. Though HFO1234yf is classified as mildly flammable, it is significantly less flammable than all HydroCarbon (HC) refrigerants and also than HFC152a and HFC32. Accordingly it can be used in direct expansion systems without a secondary loop. Nevertheless, it is recommended to minimise the refrigerant charge in order to reduce the residual risk linked to the mild flammability of HFO1234yf. The use of Brazed Plate Heat Exchangers (BPHE) instead of traditional tubular heat exchangers as evaporators and condensers in chiller and heat pumps allows a consistent reduction, one order of magnitude or more, of the refrigerant charge with no penalty in system performance.
In the open literature, it is possible to find some experimental data on HFO1234yf vaporisation and condensation heat transfer. Park and Jung (2010) compared HFO1234yf and HFC134a in nucleate boiling inside plain and low-fin tubes, whereas Saitoh et al. (2011) compared HFO1234yf and HFC134a in flow boiling inside a small diameter (2 mm) tube. Mortada et al. (2012) compared the boiling heat transfer of HFC134a and HFO1234yf at low mass fluxes inside a 6-channel tube with 1.1 mm hydraulic diameter. Del Col et al. (2010) and (2011) compared HFO1234yf and HFC134a in condensation and flow boiling inside a 1 mm diameter channel, whereas Park et al. (2011) compared HFO1234yf and HFC134a in condensation outside plain, low-fin and Turbo-C tubes. HFO1234yf shows heat transfer coefficients comparable to those of HFC134a both in condensation and vaporisation for all the heat transfer surfaces tested. Longo (2012) presented heat transfer coefficients and pressure drop measured during HFC1234yf vaporisation inside a small BPHE: HFO1234yf shows heat transfer and hydraulic performances similar to those of HFC134a.
This paper investigates the effects of saturation temperature, refrigerant mass flux and vapour super-heating on HFO1234yf condensation inside a BPHE.

*Corresponding Author

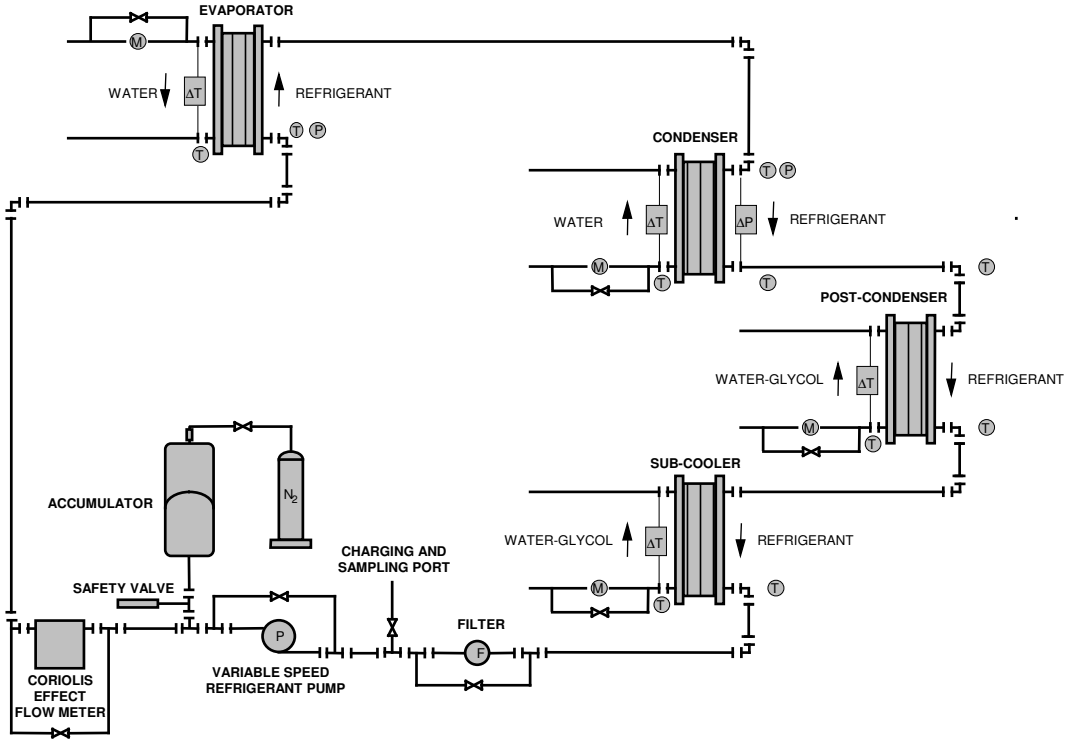

Figure 1: Schematic view of the experimental rig

2. EXPERIMENTAL SET-UP AND PROCEDURES

The experimental facility (figure 1) consists of a refrigerant loop, a water-glycol loop and two water loops. In the first loop the refrigerant is pumped from the sub-cooler into the evaporator where it is evaporated and eventually super-heated to achieve the set condition at the condenser inlet. The refrigerant flows through the condenser where it is condensed and eventually sub-cooled and then it comes back to the post-condenser and the sub-cooler. A variable speed volumetric pump sets the refrigerant flow rate and a bladder accumulator, connected to a nitrogen bottle and a pressure regulator, controls the operating pressure in the refrigerant loop. The second loop is able to supply a water-glycol flow at a constant temperature in the range of -10 to 60°C used to feed the sub-cooler and the post-condenser. The third and the fourth loops supply two water flows at a constant temperature in the range of 3 to 60°C used to feed the evaporator and the condenser respectively.

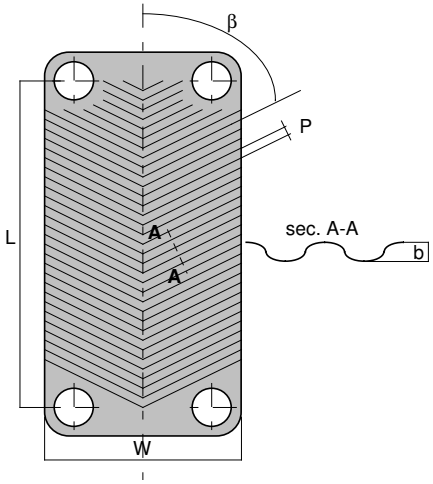

Figure 2: Schematic view of the plate

Table 1: Geometrical characteristics of the BPHE

Fluid flow plate length L(mm)	278.0
Plate width W(mm)	72.0
Area of the plate A(m^2)	0.02
Enlargement factor Φ	1.24
Corrugation type	Herringbone
Angle of the corrugation β(°)	65
Corrugation amplitude b(mm)	2.0
Corrugation pitch p(mm)	8.0
Number of plates	10
Number of effective plates N	8
Channels on refrigerant side	4
Channels on water side	5

Table 2: Specification of the different measuring devices

Device	**Type**	**Uncertainty (k= 2)**	***Range***
Thermometer	T-type thermocouple	0.1 K	-20 / 80°C
Differential thermometer	T-type thermopile	0.05 K	-20 / 80°C
Abs. pressure transducer	Strain-gage	0.075% f.s.	0 / 1.2 MPa
Diff. pressure transducer	Strain-gage	0.075% f.s.	0 / 0.3 MPa
Refrigerant flow meter	Coriolis effect	0.1% measured value	0 / 300 kg/h
Water flow meter	Magnetic	0.15% f.s.	100 / 1200 l/h

The condenser tested is a BPHE consisting of 10 plates, 72 mm in width and 310 mm in length, which present a macro-scale herringbone corrugation with an inclination angle of 65° and a corrugation amplitude of 2 mm. Figure 2 and table 1 give the main geometrical characteristics of the BPHE tested.
The temperatures of refrigerant and water at the inlet and outlet of the condenser and the evaporator are measured by T-type thermocouples (uncertainty (k= 2) within ±0.1 K); the water temperature variations through the condenser and the evaporator are measured by T-type thermopiles (uncertainty (k= 2) within ±0.05 K). The refrigerant pressures at the inlet of the condenser and the evaporator are measured by two absolute strain-gage pressure transducers (uncertainty (k= 2) within 0.075% f.s.); the refrigerant pressure drop through the condenser is measured by a strain-gage differential pressure transducer (uncertainty (k= 2) within 0.075% f.s.). The refrigerant mass flow rate is measured by means of a Coriolis effect mass flow meter (uncertainty (k= 2) of 0.1% of the measured value); the water flow rates through the condenser and the evaporator are measured by means of magnetic flow meters (uncertainty (k= 2) of 0.15% of the f.s.). All the measurements are scanned and recorded by a data logger linked to a PC: table 2 outlines the main features of the different measuring devices in the experimental rig.
Before starting each test the refrigerant is re-circulated through the circuit, the post-condenser and the sub-cooler are fed with a water glycol flow rate at a constant temperature and the condenser and the evaporator are fed with water flow rates at constant temperatures. The refrigerant pressure, vapour super-heating or vapour quality at the inlet of the condenser and the vapour quality or condensate sub-cooling at the outlet of the condenser are controlled by adjusting the bladder accumulator, the volumetric pump, the flow rate and the temperature of the water-glycol and of the water. Once temperature, pressure, flow rate and vapour quality steady state conditions are achieved at the condenser inlet and outlet both on refrigerant and water sides all the readings are recorded for a set time and the average value during this time is computed for each parameter recorded. The experimental results are reported in terms of refrigerant side heat transfer coefficients and frictional pressure drop.

3. DATA REDUCTION

The overall heat transfer coefficient in the condenser U is equal to the ratio between the heat flow rate Q, the nominal heat transfer area S and the logarithmic mean temperature difference ΔT_{ln}

$$U = Q / (S\ \Delta T_{ln}) \quad (1)$$

The heat flow rate is derived from a thermal balance on the waterside of the condenser:

$$Q = m_w\ c_{pw}\ |\Delta T_w| \quad (2)$$

where m_w is the water mass flow rate, c_{pw} the water specific heat capacity and $|\Delta T_w|$ the absolute value of the water temperature lift across the condenser. The reference heat transfer area of the condenser

$$S = N\ A \quad (3)$$

is equal to the nominal projected area $A = L \times W$ of the single plate multiplied by the number N of the effective elements in heat transfer. The logarithmic mean temperature difference is equal to:

$$\Delta T_{ln} = (T_{wo} - T_{wi}) / \ln [(T_{sat} - T_{wi})/(T_{sat} - T_{wo})] \quad (4)$$

where T_{sat} is the average saturation temperature of the refrigerant derived from the average pressure measured on refrigerant side and T_{wi} and T_{wo} the water temperatures measured at the inlet and the outlet of the condenser. The logarithmic mean temperature difference is computed with reference to the average saturation temperature on the refrigerant side without taking into account any sub-cooling or super-heating as is usual in the condenser design

procedure (Bell and Mueller, 1984). The average heat transfer coefficient on the refrigerant side of the condenser $h_{r.ave}$ is derived from the global heat transfer coefficient U assuming no fouling resistances:

$$h_{r.ave} = (1 / U - s / \lambda_p - 1 / h_w)^{-1} \quad (5)$$

by computing the water side heat transfer coefficient h_w using a modified Wilson plot technique. A specific set of experimental water to water tests is carried out on the condenser to determine the calibration correlation for heat transfer on the water side, in accordance with Muley and Manglik (1999): the detailed description of this procedure is reported by Longo and Gasparella (2007). The calibration output correlation for waterside heat transfer coefficient is:

$$h_w = 0.277 \, (\lambda_w / d_h) \, Re_w^{0.766} \, Pr_w^{0.333} \quad (6)$$

$$5 < Pr_w < 10 \qquad 200 < Re_w < 1200$$

The refrigerant vapour quality at the condenser inlet and outlet X_{in} and X_{out} are computed starting from the refrigerant temperature $T_{e.in}$ and pressure $p_{e.in}$ measured at the inlet of the evaporator (sub-cooled liquid condition) considering the heat flow rate exchanged in the evaporator and in the condenser (Q_e and Q, respectively) and the pressures p_{in} and p_{out} measured at the inlet and outlet of the condenser as follows:

$$X_{in} = f(J_{in}, p_{in}) \quad (7)$$

$$X_{out} = f(J_{out}, p_{out}) \quad (8)$$

$$J_{in} = J_{e.in} \, (T_{e.in}, p_{e.in}) + Q_e / m_r \quad (9)$$

$$J_{out} = J_{in} - Q / m_r \quad (10)$$

$$Q_e = m_{e.w} \, c_{pw} \, |\Delta T_{e.w}| \quad (11)$$

where J is the specific enthalpy of the refrigerant, m_r the refrigerant mass flow rate, $m_{e.w}$ the water flow rate and $|\Delta T_{e.w}|$ the absolute value of the temperature variation on the waterside of the evaporator. During the experimental tests with super-heated vapour inlet and sub-cooled condensate outlet, it is possible to compare the thermal balance on the water side to that on the refrigerant side of the condenser: the misbalance is always less than 4%. The refrigerant properties are evaluated by Refprop 8.0 (NIST, 2008).

The frictional pressure drop on the refrigerant side Δp_f is computed by subtracting the manifolds and ports pressure drops Δp_c and adding the momentum pressure rise (deceleration) Δp_a and the gravity pressure rise (elevation) Δp_g to the total pressure drop measured Δp_t:

$$\Delta p_f = \Delta p_t - \Delta p_c + \Delta p_a + \Delta p_g \quad (12)$$

The momentum and gravity pressure drops are estimated by the homogeneous model for two-phase flow as follows:

$$\Delta p_a = G^2 (v_G - v_L) \, |\Delta X| \quad (13)$$

$$\Delta p_g = g \, \rho_m \, L \quad (14)$$

where v_L and v_G are the specific volume of liquid and vapour phase, $|\Delta X|$ is the absolute value of the vapour quality change between inlet and outlet and

$$\rho_m = [X_m / \rho_G + (1 - X_m) / \rho_L]^{-1} \quad (15)$$

is the average two-phase density between inlet and outlet calculated by the homogeneous model at the average vapour quality X_m between inlet and outlet. The manifold and port pressure drops are empirically estimated, in accordance with Shah and Focke (1998), as follows

$$\Delta p_c = 1.5 \, G^2 / (2 \, \rho_m) \quad (16)$$

4. ANALYSIS OF THE RESULTS

Two different sets of condensation tests with refrigerant HFO1234yf down-flow and water up-flow are carried out at four different saturation temperatures: 25, 30, 35 and 40°C. The first set includes 42 saturated vapour tests in which the inlet vapour quality varies between 0.95 and 1.00 and the outlet vapour quality between 0.00 and 0.09. The

second set includes 42 tests with super-heated (from 9.4 to 10.9 K) vapour inlet and sub-cooled (from 0.0 to 1.6 K) condensate outlet as it occurs in chiller and heat pump applications. Table 3 shows the experimental tests operating conditions: refrigerant saturation temperature T_{sat} and pressure p_{sat}, inlet and outlet refrigerant vapour quality X_{in} and X_{out}, inlet vapour super-heating ΔT_{sup} and outlet condensate sub-cooling ΔT_{sub}, refrigerant mass flux G_r and heat flux q. A detailed error analysis performed in accordance with Kline and McClintock (1954) indicates an overall uncertainty within ±12% for the refrigerant heat transfer coefficient measurement and within ±18 % for the refrigerant total pressure drop measurement.

Figure 3 shows the average heat transfer coefficients on the refrigerant side vs. refrigerant mass flux for saturated vapour and super-heated vapour condensation at different saturation temperatures (25, 30, 35 and 40°C). The heat transfer coefficients show weak sensitivity to saturation temperature. The saturated vapour data and the super-heated vapour data show the same trend vs. refrigerant mass flux. At low refrigerant mass flux (< 20 kg/m^{2}s) the heat transfer coefficients are not dependent on mass flux and probably condensation is controlled by gravity. For higher refrigerant mass flux (> 20 kg/m^{2}s) the heat transfer coefficients depend on mass flux and forced convection condensation occurs. In the forced convection condensation region a doubling of the refrigerant mass flux (from 20 to 40 kg/m^{2}s) involves a 32-36% enhancement in the heat transfer coefficient (from 1600 to 2200 W/m^{2}K for saturated vapour and from 1750 to 2300 W/m^{2}K for super-heated vapour condensation). The super-heated vapour heat transfer coefficients are from 8 to 11% higher than those of saturated vapour under the same refrigerant mass flux.

Vapour super-heating affects condensation kinetics reducing the condensate film thickness and increasing the heat transfer coefficient with respect to saturated vapour as demonstrated by Fujii (1991) and by Mitrovic (2000) for laminar film condensation and by Webb (1998) for forced convection condensation. Present experimental results for refrigerant HFO1234yf are in fair agreement with those previously obtained by one of the present authors for HFC and HC refrigerants (Longo, 2008, 2009, 2011).

The saturated vapour condensation heat transfer coefficients have been compared against the classical Nusselt (1916) analysis for laminar film condensation on vertical surface and the Akers et al. (1959) equation for forced convection condensation inside a tube.

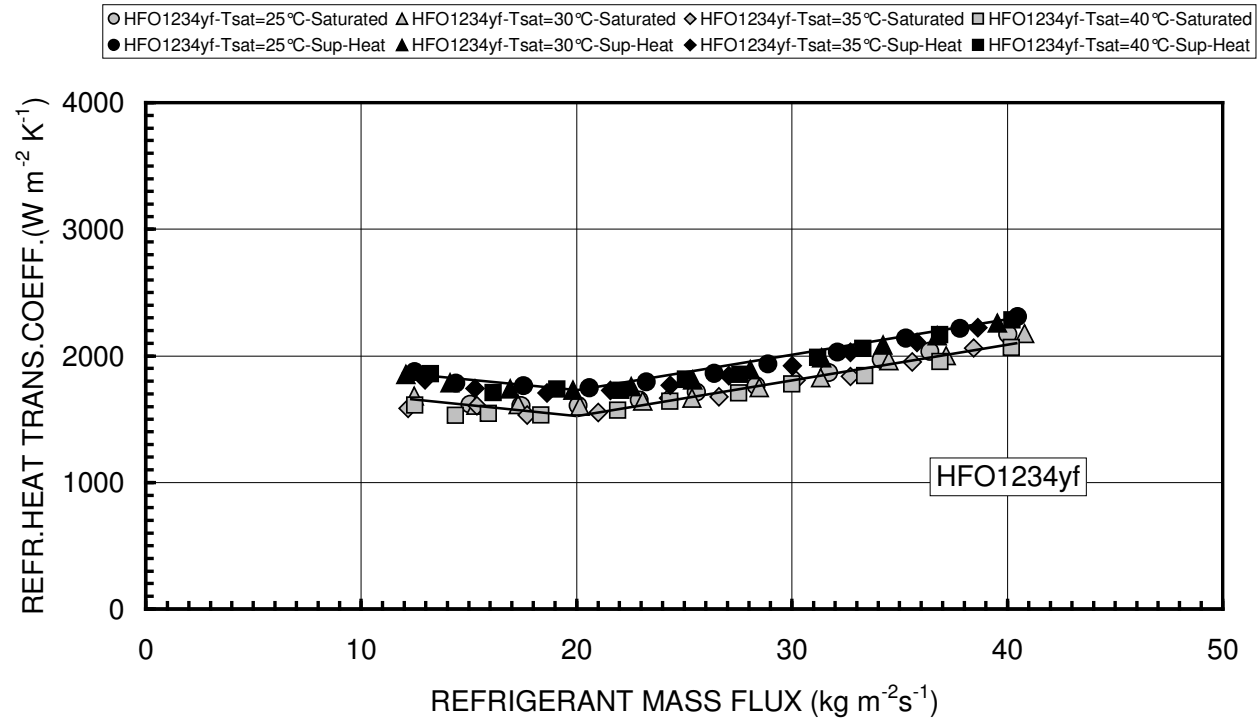

Figure 3: Average heat transfer coefficient on refrigerant side vs. refrigerant mass flux

Table 3: Operating conditions during experimental tests

Set	Runs	T_{sat} (°C)	p_{sat} (MPa)	X_{in}	X_{out}	ΔT_{sup} (K)	ΔT_{sub} (K)	G_r (kg/m^{2}s)	q (kW/m^2)
1st	42	24.9–40.2	0.68–1.02	0.95–1.0	0.0–0.09	=	=	11.0–40.8	5.3–21.0
2nd	42	24.9–40.1	0.68–1.02	=	=	9.4–10.9	0.0-1.6	12.1–40.5	6.7–23.2

The Nusselt (1916) analysis is valid for gravity controlled laminar film condensation: the average heat transfer coefficient on the vertical surface results

$$h_{NUSSELT} = 0.943 \left[(\lambda_L^3 \rho_L^2 g \Delta J_{LG}) / (\mu_L \Delta T L)\right]^{1/4} \quad (17)$$

where ρ_L, λ_L and μ_L are the condensate density, thermal conductivity and dynamic viscosity respectively, ΔJ_{LG} is the specific enthalpy of vaporisation, g is the gravity acceleration, ΔT the difference between saturation and wall temperature and L the length of the vertical surface. This equation has been multiplied by the enlargement factor Φ (equal to the ratio between the actual area and the projected area of the plates) to compute the heat transfer coefficient inside the BPHE referred to the projected area of the plates

$$h_{r.ave} = \Phi \, h_{NUSSELT} \quad (18)$$

The enlargement factor Φ for the BPHE tested is equal to 1.24.
The Akers et al. (1959) equation developed for forced convection condensation inside tube results

$$h_{AKERS} = 5.03 \, (\lambda_L / d_h) \, Re_{eq}^{1/3} \, Pr_L^{1/3} \quad (19)$$

where

$$Re_{eq} = G \left[(1 - X) + X \, (\rho_L / \rho_G)^{1/2}\right] d_h / \mu_L \quad (20)$$

$$Pr_L = \mu_L \, c_{pL} / \lambda_L \quad (21)$$

are the equivalent Reynolds number and the Prandtl number respectively. This equation, valid for $Re_{eq} < 50000$, gives the local heat transfer coefficient which has been multiplied by the enlargement factor Φ and integrated by a finite difference approach along the heat transfer area to compute the average condensation heat transfer coefficient inside BPHE referred to the projected area of the plates

$$h_{r.ave} = (1 / S) \int_0^S \Phi \, h_{AKERS} \, dS \quad (22)$$

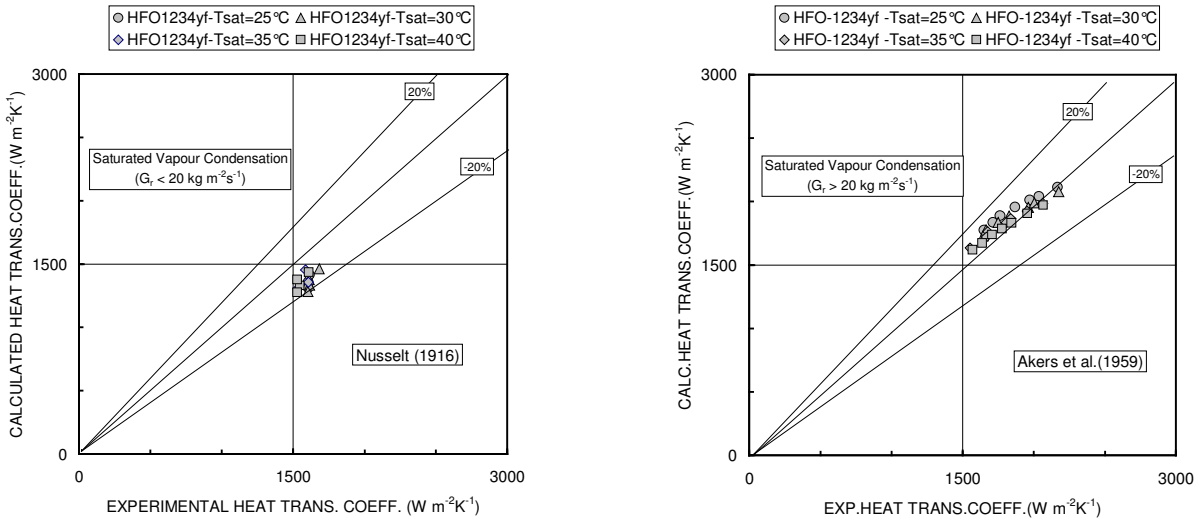

a) Nusselt (1916) equation b) Akers et al.(1959) equation

Figure 4: Comparison between experimental and calculated saturated vapour heat transfer coefficients

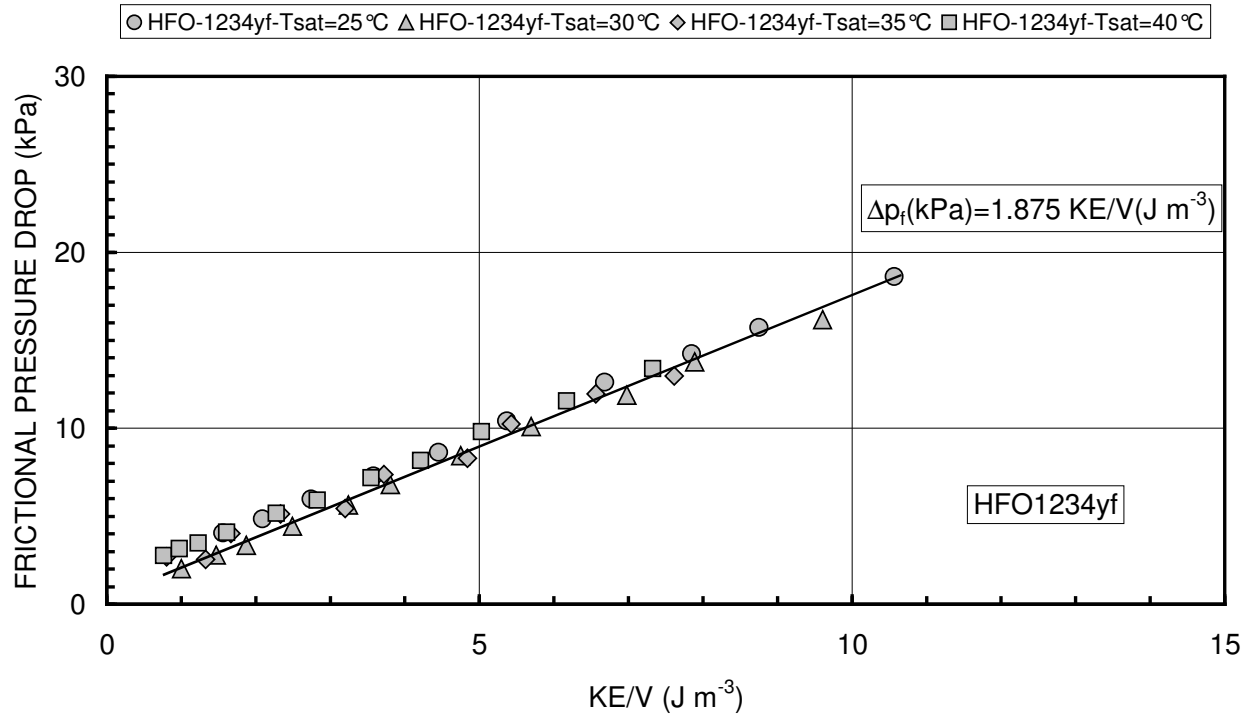

Figure 5: Frictional pressure drop vs. kinetic energy per unit volume

Figure 4a shows the comparison between the saturated vapour condensation heat transfer coefficients at low refrigerant mass flux (G_r < 20 kg/m^{2}s) and the average heat transfer coefficients calculated by Nusselt (1916) (eq.18). Figure 4b shows the comparison between the saturated vapour condensation heat transfer coefficients at high refrigerant mass flux (G_r > 20 kg/m^{2}s) and the average heat transfer coefficients calculated by Akers et al. (1959) (eq.22). The Nusselt (1916) equation reproduces the saturated vapour condensation data at low refrigerant mass flux with an absolute mean percentage deviation of 14.4%. Akers et al. (1959) model predicts the saturated vapour condensation data at high refrigerant mass flux with an absolute mean percentage deviation of 3.4%.
Figure 5 shows the saturated vapour condensation frictional pressure drop against the kinetic energy per unit volume of the refrigerant flow computed by the homogeneous model:

$$KE/V = G^2 /(2\,\rho_m) \tag{23}$$

The frictional pressure drop shows a linear dependence on the kinetic energy per unit volume of the refrigerant flow and therefore a quadratic dependence on the refrigerant mass flux. The following best fitting equation has been derived from present experimental data:

$$\Delta p_f = 1.875\ KE/V \tag{24}$$

This correlation reproduces present experimental data with a mean absolute percentage deviation around 12.3%.
HFO1234yf is a candidate substitute for HFC134a in air conditioning systems and most users are looking to HFO1234yf as a drop-in solution. Therefore it is interesting to compare the heat transfer and hydraulic performances of HFO1234yf refrigerant to those of HFC134a. The present HFO1234yf condensation heat transfer coefficients and frictional pressure drop have been compared with those of HFC134a previously measured by Longo (2008) inside the same BPHE under the same operating conditions. HFO1234yf exhibits heat transfer coefficients lower (10-12%) and frictional pressure drop lower (10-20%) than those of HFC134a under the same operating conditions.

5. CONCLUSIONS

This paper investigates the effects of refrigerant mass flux, saturation temperature and vapour super-heating on heat transfer and pressure drop during HFO1234yf condensation inside a commercial BPHE. The heat transfer coefficients show weak sensitivity to saturation temperature and great sensitivity to refrigerant mass flux. The

transition between gravity controlled and forced convection condensation occurs at a refrigerant mass flux around 20 kg/m^{2}s. In the forced convection condensation region the heat transfer coefficients show a 32-36% enhancement for a doubling of the refrigerant mass flux. The super-heated vapour condensation heat transfer coefficients show the same trend of saturated vapour data vs. refrigerant mass flux with values from 8 to 11% higher under the same refrigerant mass flux.

The frictional pressure drop shows a linear dependence on the kinetic energy per unit volume of the refrigerant flow and therefore a quadratic dependence on the refrigerant mass flux.

The heat transfer coefficients for saturated vapour are sufficiently well predicted by the Nusselt (1916) analysis for vertical surface in the gravity controlled region and by the Akers et al. (1959) model in the forced convection region.

A linear equation based on the kinetic energy per unit volume of the refrigerant flow is proposed for the computation of frictional pressure drop.

HFO1234yf exhibits heat transfer coefficients lower (10-12%) and frictional pressure drop lower (10-20%) than those of HFC134a under the same operating conditions.

REFERENCES

Akers, W.W., Deans, H.A., Crosser, O.K., 1959, Condensing heat transfer within horizontal tubes, *Chem. Eng. Prog. Symp. Series*, vol. 55, p. 171-176.

Bell, K.J., Mueller, A.C., 1984, *Wolverine Heat Transfer Data Book*, Wolverine, p. 163-165.

Del Col, D., Torresin, D., Cavallini, A., 2010, Heat transfer and pressure drop during condensation of the low GWP refrigerant R1234yf, *Int. J. Refrig.*, vol. 33, p. 1307-1318.

Del Col, D., Bortolin, S., Torresin, D., Cavallini, A., 2011, Flow boiling of R1234yf in a 1 mm diameter channel, Proc. of 23rd Int. Congress of Refrigeration, Prague, Czech Republich.

Fujii, T., 1991, *Theory of laminar film condensation*, Springer, Berlin, p. 75-81, 83-87.

Kline, S.J., McClintock, F.A., 1954, Describing uncertainties in single-sample experiments, *Mech. Eng.*, vol. 75, p. 3-8.

Longo, G.A., Gasparella, A., 2007, Heat transfer and pressure drop during HFC refrigerant vaporisation inside a brazed plate heat exchanger, *Int. J. Heat Mass Transfer*, vol.50, p. 5194-5203.

Longo, G.A., 2008, Refrigerant R134a condensation heat transfer and pressure drop inside a small brazed plate heat exchanger, *Int. J. Refrig.* vol. 31, p. 780–789

Longo, G.A., 2009, R410A condensation inside a commercial brazed plate heat exchanger, *Exp. Therm. Fluid Science*, vol. 33, p. 284–291.

Longo, G.A., 2011, The effect of vapour super-heating on hydrocarbon refrigerant condensation inside a brazed plate heat exchanger, *Exp. Therm. Fluid Science*, vol. 35, p. 978–985.

Longo, G.A., 2012, Vaporisation of the low GWP refrigerant HFO1234yf inside a brazed plate heat exchanger, *Int. J. Refrig.,* In Press.

Mitrovic, J., 2000, Effects of vapour superheating and condensate subcooling on laminar film condensation, ASME *J. Heat Transfer*, vol. 122, p. 192-196.

Mortada, S., Zoughaib, A, Arzano-Daurelle, C., Clodic, D., 2012, Boiling heat transfer and pressure drop of R-124a and R-1234yf in minichannels for low mass fluxes, *Int. J. Refrig.*, In Press

Muley, A., Manglik, R.M., 1999, Experimental study of turbulent flow heat transfer and pressure drop in a plate heat exchanger with chevron plates, *ASME J. Heat Transfer*, vol. 121, p. 110-121.

NIST, 2008, *Standard Reference Database, REFPROP 8.0.*

Nusselt, W., 1916, Die oberflachenkondensation des wasserdampfes, *Z. Ver. Dt Ing.*, vol. 60, p. 541-546, 569-575.

Park, K-J., Jung, D., 2010, Nucleate boiling heat transfer coefficients of R1234yf on plain and low fin surfaces, *Int. J. Refrigeration*, vol. 33, p. 553-557.

Park, K-J., Kang, D.G., Jung, D., 2011, Condensation heat transfer coefficients of R1234yf on plain, low fin, and Turbo-C tubes, *Int. J. Refrig.*, vol. 34, p. 317-321

Saitoh, S., Dang, C., Nakamura, Y., Hihara, E., 2011, Boiling heat transfer of HFO-1234yf flowing in a smooth small-diameter horizontal tube *Int. J. Refrig.*, vol. 34, p. 1846-1853.

Shah, R.K., Focke, W.W., 1988, Plate heat exchangers and their design theory, *In*: Subbarao E.C., Mashelkar R.A., *Heat Transfer Equipment Design*, Hemisphere, Washington, p. 227-254.

Webb, R.L., 1998, Convective condensation of superheated vapor, *ASME J. Heat Transfer*, vol. 120, p. 418-421.